Proc Indian Natn Sci Acad **79** No. 4 December 2013 Spl. Issue, Part A, pp. 825-828
© *Printed in India.*
DOI: 10.16943/ptinsa/2013/v79i4/48009

Research Paper

X-Ray Tomography Based Observations on Interfacial Behavior of 3D Carbon/Carbon Composite

R SHARMA[1*], P MAHAJAN[2] and R K MITTAL[3]
Department of Applied Mechanics, Indian Institute of Technology Delhi, New Delhi 110 016, India

(Received 30 January 2013; Accepted 09 March 2013)

Fiber bundle Pull-out test was conducted for the interfacial characterization of 3D carbon/carbon (C/C) composite. The specimens of the composite were reconstructed using X-ray tomography before and after the testing. The interfacial cracks and their propagation had been clearly revealed from the reconstructed 2D images of the specimens. The bundle/matrix interfaces in C/C composite were observed damaged initially and application of the load changed the configuration of these cracks. Some cracks at the interfaces closed and some opened during the loading history. The debonded surfaces were highly rough and contributed to a high frictional force. The bundle/matrix interfacial properties such as interfacial shear strength, fracture energy release rate and debond strength in the bundle were obtained as 3.8 MPa, 4.7 N/m and 83MPa.

Key Words: Pull-out Test; X-ray Tomography; Fracture Energy Release Rate; Interfacial Parameters

1. Introduction

C/C composites experience high thermal stresses during the graphitization and cooling process. During the manufacturing process most of the interfaces in composite and matrix got damaged and it is generally accepted that fibre bundle/matrix interface has a significant influence on the fracture and mechanical behaviour of the composites [1-2]. The properties of the bundle/matrix interface such as interfacial shear strength and fracture energy are required to model the interfacial behaviour of these constituents in the finite element simulations. The fiber bundle pull-out and push-out tests are commonly conducted and cited in the literature for interfacial characterization. The load-displacement data obtained from these tests was fitted to the analytical shear-lag models to obtain the interfacial parameters [3-5]. Here, the approach of Sakai et al. [6] was used to obtain the interfacial parameters for bundle/matrix interface and the fracture process of the interface was observed using X-ray tomography images. Earlier authors had used the X-ray tomography to explore the internal material damage in the 3D C/C composite [7-9]. In the present work the specimens were scanned before and after the testing, and reconstructed 2D images were compared to observe the fracture process of the bundle/matrix interface in the composite.

2. Materials

C/C composite under investigation has 3D hybrid architecture, which consists of rectangular bundles in x and y directions and circular bundles in z directions as shown in Fig. 1. The rectangular bundles made of 24,000 fibers and circular rods made of 15,000 fibers. The composite was prepared using pitch based matrix impregnation technique and the graphitization temperature was nearly 2200°C. The specimens were prepared in the form of prismatic rods from the random locations in the composite. The specimen details are shown in the Fig. 1.

*Authors for Correspondence: E-mail: [1]*rajnish0007@gmail.com*, [2]*mahajan@am.iitd.ernet.in*, [3]*rkm@am.iitd.ac.in*

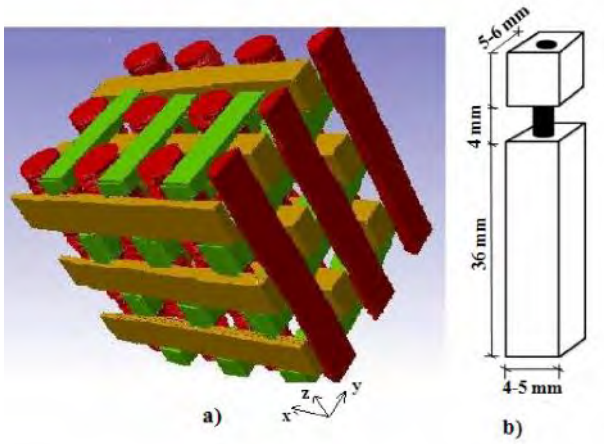

Fig. 1: a) Architecture of composite and b) Schematic diagram of pull-out test specimen

(a) X-ray Tomography of Composite

Computed tomography (CT) scan facility available at Snow and Avalanche Study Establishment at Manali, India, was utilized for the X-ray tomography experiments. It consists of a fan type X-ray source and can scan up to 2 μm resolution. The scanning details of the composite are given in Table 1. The defects observed in the reconstructed images of composite from X-ray tomography were earlier discussed in detail by authors [9]. The cracks originated during the manufacturing process were divided into three families according to their location of presence: Bundle/matrix interfacial cracks, intra-bundle cracks, and matrix cracks. Intra-bundle cracks originated either due to the shrinkage stresses or due to the high temperature treatment during the graphitization process of composite. The generation of bundle/matrix interfacial cracks was predominantly due to the high thermal stresses generated due to the mismatch between the thermal expansion coefficients of fiber bundle and matrix. The matrix cracking was due to shrinkage stresses generated during the cooling process. The bundle/matrix interfacial cracks were further classified as 1) Cracks propagating through bundle/matrix interface, 2) Cracks propagating through matrix and merging with the voids or joining the transverse cracks and 3) Cracks partly propagating through matrix and returning to the interface [9]. These cracks also propagated up to 50% in periphery at many locations along the length of bundle. The micro pores were also present in the matrix along the cracks. The big air cavities present in the matrix pockets were nearly periodically distributed in the composite. The structural model index of these voids was near to 3, which corresponds to spherical in shape [9].

Table 1. Scanning details for the specimens

Voltage (kV)	Current (mA)	Angular displacement (°)	Exposure time (ms)	Pixel size (μm)
80 100	0.30	1178	6.9	

The composite specimens of pull out test scanned before and after testing to have an idea of the propagation of the interfacial cracks. Fig. 2(a) shows the pretest scanned 2D image and Fig. 2(b) shows the posttest scanned 2D images of the same specimen at same location. The network of the cracks can be observed partially developed in the composite as shown in Fig. 2a. The fiber bundle at the centre in Fig.2 was subjected to the pull-out forces.

Fig. 2a reveals the partial propagation of the interfacial cracks in the composite. Some micro-voids were observed near the bundle/matrix interfaces. The network of the interfacial cracks after failure can be summarised from Fig. 2b. As the load was applied on the bundle, interfacial cracks configuration in the composite had changed. Some cracks opened up and a few were closed due to the lateral movement of the bundle (ref. Red rectangles marked in Fig. 2). The interfacial crack propagated nearly from the fiber bundle/matrix interfaces as clearly revealed in Fig. 2b. At some locations, bundle was closely packed with matrix due to the roughness of the surface and misalignment of bundle, therefore the region looks like as a bonded region (see the area within the rectangles Fig. 2b). These types of regions had contributed to the frictional forces during the sliding process of bundle after interfacial failure. At a few locations the interfacial cracks propagated and merged with micro-voids as shown in Fig. 2b (see the area within the circle). The overall phenomenon of the cracking was very complex and can be summarized as a mixed mode failure at local level. The pre-existence of cracks, micro-pores, roughness and misalignment of bundles gave rise to multi-mode failures at local levels

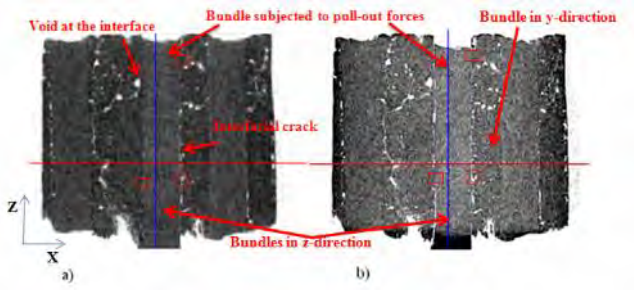

Fig. 2: 2D CT images of the pull-out specimen a) before and b) after testing

as some cracks were in opening mode and some were in closing mode. Although, globally this fracture process can be treated as mode-II failure and the resistance against the pull-out force was due to the contribution of cohesiveness and anchorage between the bundle/matrix surfaces.

(b) Fiber Bundle Pull-out Test

The experiments were performed on universal testing machine with a load cell of 5kN at a low strain rate 0.01 mm/min. The fiber bundle was pulled out of the composite in tensile loading. The typical load displacement curve is shown in Fig. 3. The load was increased nonlinearly up to the peak as shown in Fig. 3. The nonlinearity in the curve was due to the progress in debonding at the interface. A sudden drop in load drop was observed after the peak load which confirmed the total debonding of the interface. The drop in load was nearly 25% of the peak load due to sudden failure. The post peak curve stabilized after a short duration with a gentle decreasing slope. The load drop was observed nearly 50% at the stabilization. This was due to the high frictional forces present between the debonded surfaces of bundle/matrix interfaces. The roughness of debonded surfaces causes a very high friction due the anchorage effect. The further reduction in the fictional force was due to the abrasion of the debonded surfaces and reduction in the contact area of bundle during the sliding process.

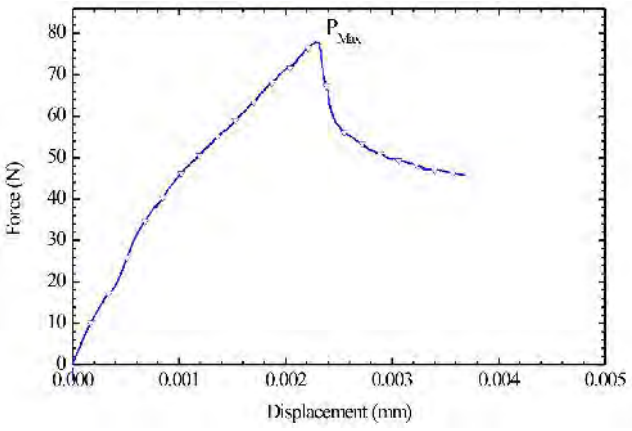

Fig. 3: Typical load-displacement curve of pull-out test

(c) Interpretation of the Parameters

The fracture energy release rate and debond shear strength were calculated using analytical approach of Sakai *et al.* [6]. In this approach, it was assumed that the crack will start and grow along the periphery of the fiber bundle and critical load P_{max} at the onset of delamination defines the critical stress. The critical debond axial stress in bundle σ_{max} was calculated by dividing the maximum load with cross sectional area of the bundle.

$$\sigma_{max} = \frac{P_{max}}{A_d} \tag{1}$$

Here, $A_d = (\pi D^2/4)$ is the cross-sectional area of the bundle and D is the diameter of the fiber bundle. The compliance of the debonded bundle C_d can be expressed as given in Eq. 2 by neglecting friction at the interface [6].

$$C_d = \frac{l_d}{\pi r^2 E} \tag{2}$$

Here, l_d is the debond length. Here, E is the Young's modulus of the fiber bundle in longitudinal direction and was taken as 240 GPa. The critical energy release rate (G_{IIc}) can be expressed as given below in Eq. 3.

$$G_{IIC} = \left(\frac{P_{max}^2}{2}\right)\left(\frac{\partial C_d}{\partial A_d}\right) = \frac{2P_{max}^{\ 2}}{\pi^2 D^3 E} \tag{3}$$

The average shear strength was calculated from the maximum load under the assumption that shear stress was uniformly distributed along the interface and is given by Eq. 4.

$$\tau = \frac{P_{max}}{\pi r l_d} \text{ MPa} \quad (4)$$

The obtained interfacial shear strength, normal stress in bundle, and fracture energy release rate are given with associated uncertainties in Table 2. The

Table 2: Interfacial parameters of bundle/matrix interface

Test	Shear strength τ N/mm^2	Normal strength σN/mm^2	Fracture energy release rate G_{IIC} N/m
Pull out	3.80 ± 0.52	83.12± 11.2	4.73± 1.24

mean shear and normal strengths of the interface are 3.8 N/mm^2 and 83.12 N/mm^2 respectively. The energy release rate in the mode II is obtained as 4.73 N/m. The obtained parameters of the bundle/matrix interface can be used in the finite element analysis of the composite to study its overall mechanical behavior. The above study is concluded in the nest section.

3. Conclusions

Fiber bundle pull-out tests were conducted to obtain the interfacial parameters for the bundle/matrix interface. X-ray tomography was used to reconstruct the material damage in the micro-structure of the composite. The specimens were scanned using X-ray tomography and phenomenon of the interfacial crack propagation during the pull-out test was explored from the 2D reconstructed images. The presence of the artifacts had given rise to multi-mode failures at local levels, however the failure can be considered as in mode-II globally. Finally, the interfacial shear and normal strengths, and fracture energy release rate in mode-II were obtained from load-displacement curves.

4. Acknowledgement

The authors are grateful to Snow and Avalanche Study Establishment (SASE), Manaly for providing access to X-ray tomography facility.

References

1. Jortner J *Carbon* **24** (1986) 603-613
2. Rao V M, Mahajan P and Mittal R K *Composite Interfaces* **15** (2008) 379-409
3. Hutchinson J W and Jenesen H M Models of fiber debonding and pull-out in brittle composites with friction *Mechanics of Materials* **9(2)** (1990) 139-163
4. Domnanovich A, Peterlik H and Kromp K *Composites Science and Technology* **56** (1996) 1017-1029
5. Aoki T, Yamane Y, Ogasawara T, Ogawa T, Sugimoto S and Ishikawa T *Carbon* **45** (2007) 459-467
6. Sakai M, Matsuyama R and Miyajima T *Carbon* **38** (2000) 2123-2131
7. Sharma R, Mahajan P and Mittal R K *Carbon* **50** (2012) 2717-2725
8. Sharma R, Mahajan P and Mittal R K *Composite Structure* (2012) Available online 5 December 2012
9. Sharma R, Mahajan P and Mittal R K *Submitted to Carbon* (2012).